

# High-Energy Radiation-Resistant Vulcanizates. II. EPDM

CHAITANYA S. SHAH,<sup>1</sup> MAHENDRA J. PATNI,<sup>1</sup> and MADHAV V. PANDYA<sup>2,\*</sup>

<sup>1</sup>Materials Science Centre and <sup>2</sup>Chemistry Department, Indian Institute of Technology, Powai, Bombay 400 076, India

## SYNOPSIS

In this article, Part II of the series, we report a detail study on stabilization of EPDM vulcanizates in  $\gamma$ -radiation environment. The special additives (antirads), namely pyrene (Py), brominated acenaphthene (BrAc), poly(acenaphthene sulfide) (PACSu) and poly(pyrene sulfide) (PPySu) were used for the stabilization studies. The efficiency of these antirads for EPDM had been monitored by the means of electrical resistivity, wide-angle X-ray diffraction, and mechanical properties. The stabilization of EPDM to withstand 200 Mrads of  $\gamma$  radiation in air environment is achieved. © 1994 John Wiley & Sons, Inc.

## INTRODUCTION

The flexible, tough, dielectric elastomeric materials are used for various applications such as gaskets, seals, vibration dampers, belts, insulations, etc. One of the widely used synthetic elastomer for such applications in recent years is ethylene propylene diene terpolymer (EPDM) because of its easy processability and very good thermo-mechanical and electrical properties. The ethylene and propylene contribute up to 95% of the total monomers and govern the morphology in EPDM. The remaining 5% is the diene monomer that provides the necessary sites for crosslinking reactions. Different grades of EPDM are available with varying ratio of ethylene to propylene covering a range of performance properties.<sup>1,2</sup>

Such a versatile material can also be made useful in nuclear radiation environment because of its unique chemical composition. EPDM is reported to have better radiation resistance than other elastomeric materials.<sup>3-5</sup>

It is reported that the addition of aromatic compounds can further retard the radiation effect.<sup>6-8</sup> In our previous studies we also have shown the importance of special additives such as antirads in high-energy radiation-resistant elastomeric vulcanizates.<sup>9,10</sup> The schematics of radio-chemical changes taking place in the polymer on exposure to  $\gamma$  radia-

tion is presented in Figure 1. In this article we are reporting a detail study of variation in antirad formulation for EPDM to achieve the stability to withstand 200 Mrads of  $\gamma$  radiation in oxidative environment.

## EXPERIMENTAL WORK

### Materials

Materials used in the study with their chemical structures and sources are described in the Table I. Solvents were obtained locally and used after fractional distillation. All the other materials were obtained locally and used as received. Antirads used in this study, viz. brominated acenaphthene (BrAc), poly(acenaphthene sulfide) (PACSu) and poly(pyrene sulfide) (PPySu), were synthesized from acenaphthene and pyrene.<sup>10</sup>

### Compounding and Molding

Compounding of EPDM was carried out with necessary ingredients, as per the compositions given in Table II, on the open roller mill at 120°C. The test slabs of 15 × 15 × 0.2 cm were molded using the flywheel-type press at 160°C and 7 tonnes of pressure for optimum cure time determined from Monsanto Rheometer MDR 90 (Table III).

Specimens of 1 × 2.5 × 0.2 cm for wide-angle X-ray diffraction studies, 6.5 cm diameter discs for resistivity measurements, and dumbbells for tensile properties were cut from the test slabs.

\* To whom correspondence should be addressed.

## HIGH ENERGY DEGRADATION MECHANISM - A SCHEMATIC REPRESENTATION

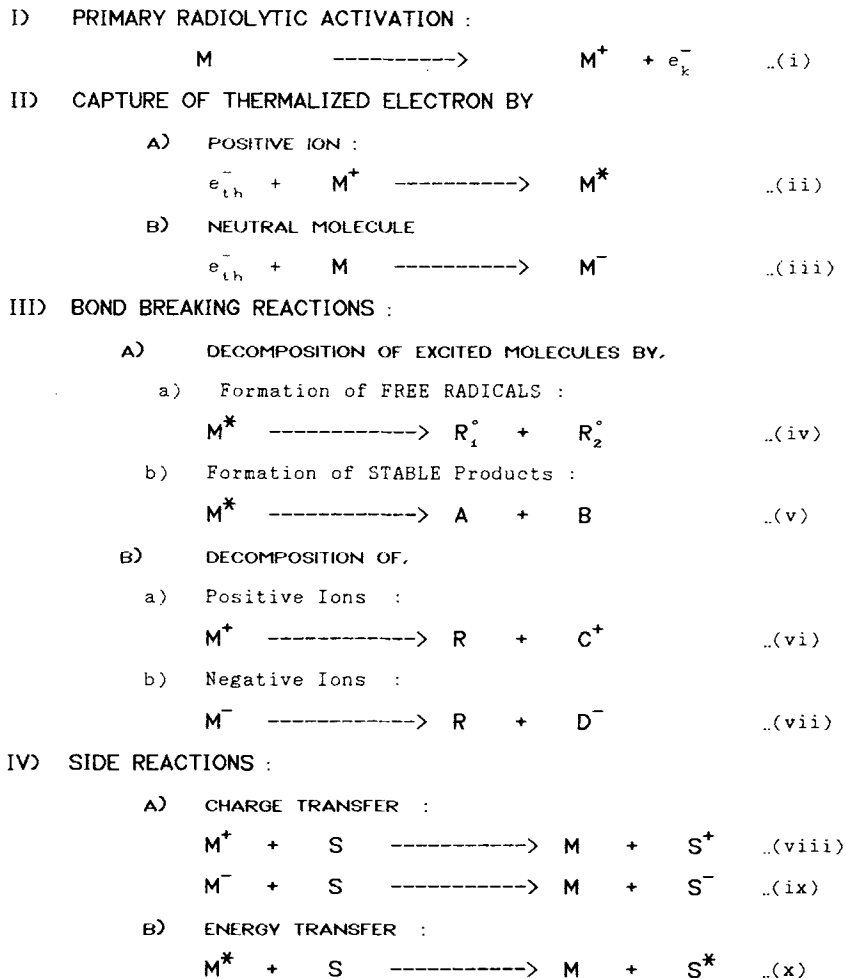


Figure 1 High-energy degradation mechanism: a schematic representation.

### Exposure Conditions

All the specimens were subjected to the  $\gamma$ -radiation exposure at 40°C in a Co<sup>60</sup> radiation facility at dose rate of 0.32 Mrads/h with continuous air flow at the approximate rate of 10 mL/min. This ensured the homogeneous effect in the bulk throughout the exposure.

### Testing Procedures

#### Volume and Surface Resistivity

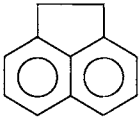
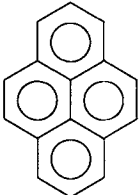
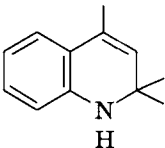
The resistivity measurements were carried out using high-resistance meter HP 4329a on the disk specimen. The measurements were carried out before as well as after  $\gamma$  irradiation of varying cumulative dosage. Time-domain measurements were carried

out after 2 Mrad  $\gamma$  irradiation, over a period of 120 h at various intervals in air.

#### Wide-Angle X-ray (WAX) Diffraction Spectroscopy

Specimens were removed from the  $\gamma$  chamber followed by conditioning at room temperature for 1 h before subjecting them to the WAX diffraction studies using  $k_\alpha$  line of Cu target ( $\lambda = 1.54060 \text{ \AA}$ ) with a monochromator, on the Philips PW 1820 diffractometer. Specimens were carefully inserted back in the  $\gamma$  chamber after each scanning. To quantify the extent of damage caused due to  $\gamma$  radiation, same specimens were used with the assumption that there would be very little effect of X-rays on the specimens during scanning.

**Table I Source and Chemical Structure of the Chemicals Used**

Name	Source	Chemical Structure
Acenaphthene	Aldrich Chemicals	
Pyrene	Fluka	
ARD Resin	Bayer India Ltd.	

**Mechanical Properties**

Mechanical properties such as tensile strength, modulus, elongation at break, and hardness were measured as per the appropriate procedures described by ASTM.

**RESULTS AND DISCUSSIONS****Surface and Volume Resistivity**

Two types of resistivity measurements were carried out to study the changes due to  $\gamma$ -radiation exposure. (a) Time-domain measurements that provided the indirect method of monitoring the rate of depletion for the transient charge species after removal from the radiation environment. (b) The extent of changes in electrical property by monitoring the

**Table II Recipe of EPDM Vulcanizates**

Material	Quantity (gm)
Ethylene propylene diene terpolymer (Royalene 552)	100.0
Paraffin wax	4.0
China clay	30.0
Aluminum silicate	40.0
Carbon black SRF	5.0
ARD resin	4.0
Sulfur	2.0
TMTD	1.0
Stearic acid	1.0
Zinc oxide	2.0
Antirad <sup>a</sup>	4.0

<sup>a</sup> Following antirads were used; recipe 1, control—no antirad; recipe 2, BrAc—brominated acenaphthene; recipe 3, Py—pyrene; recipe 4, PAcSu—poly(acenaphthene sulfide); recipe 5, PPySu—poly(pyrene sulfide).

steady-state value of resistivity with respect to the total exposed dose of  $\gamma$  radiation.

**Time-Domain Measurements**

As seen from Figure 2 [(a) and (b)], the resistivities for all the specimens are increasing with respect to time. These clearly indicate that the transient charge species formed during irradiation get depleted due to recombination or quenching mechanism.<sup>11</sup> The observed increase in resistivities follow the first-order kinetics for all the specimens. However, depending on the antirad used, the rate of increase and the final steady value reached, show a pronounced variation. The trend in the half-life data (Table IV) computed from these data representing the depletion rate of transient charge species for different antirad is as follows:

$$\text{PPySu} \sim \text{PAcSu} > \text{Py} > \text{BrAc} > \text{Control}$$

**Table III Rheometric Data EPDM Vulcanizates**

Recipe No.	Minimum Torque (dN m)	Maximum Torque (dN m)	Induction Time (min)	Scorch Time (min)	Optimum Cure Time (min)
1	10	69	2.0	4.0	22.5
2	9	66	1.8	4.5	23.0
3	8	68	2.0	4.5	23.0
4	10	67	1.8	4.2	22.5
5	9	68	1.8	4.2	22.5

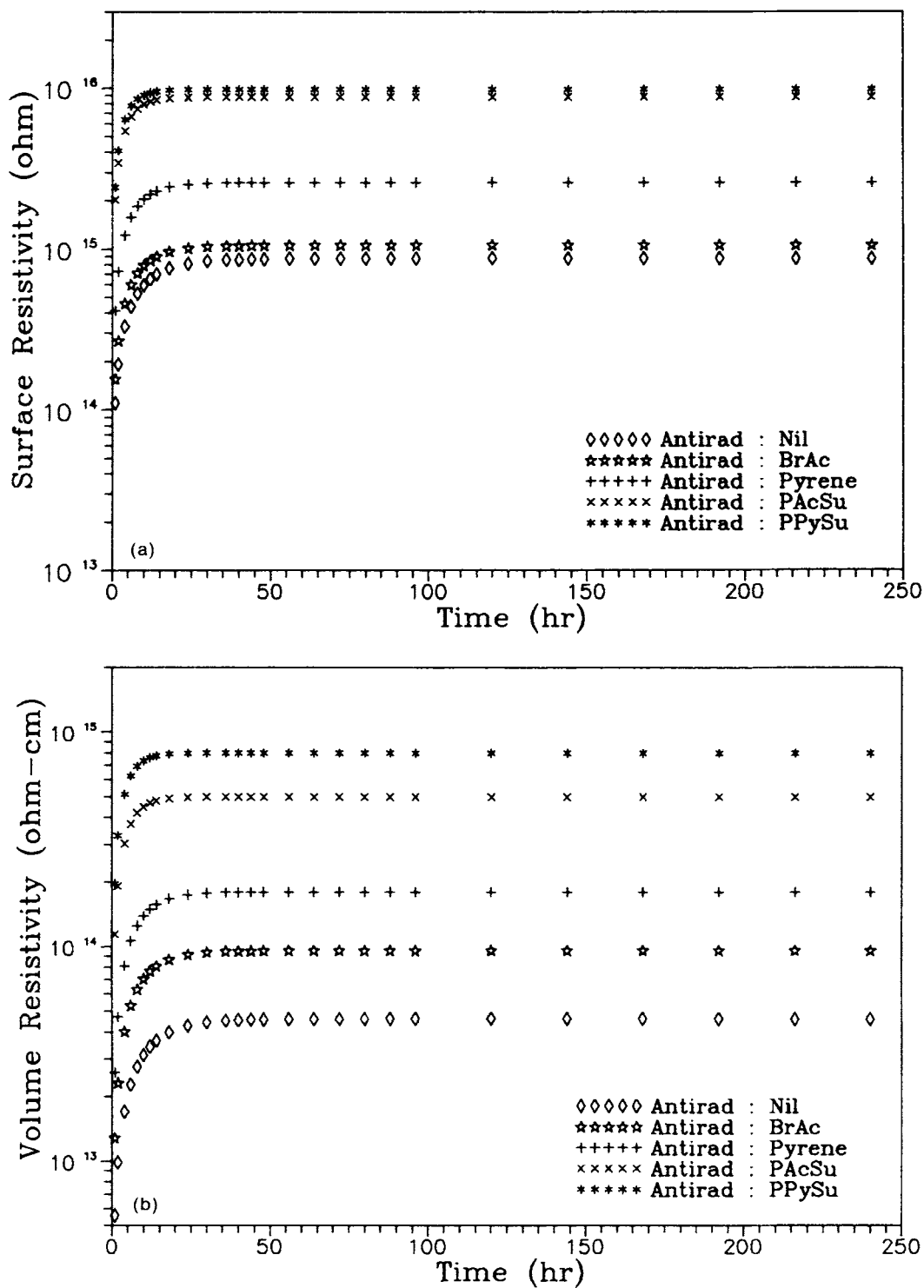


**Figure 2** (a) Plots of surface resistivity in time-domain measurements for EPDM vulcanizates after exposure to 2.0 Mrad exposure in  $\gamma$  radiation. (b) Plots of volume resistivity in time-domain measurements for EPDM vulcanizates after exposure to 2.0 Mrad exposure in  $\gamma$  radiation.

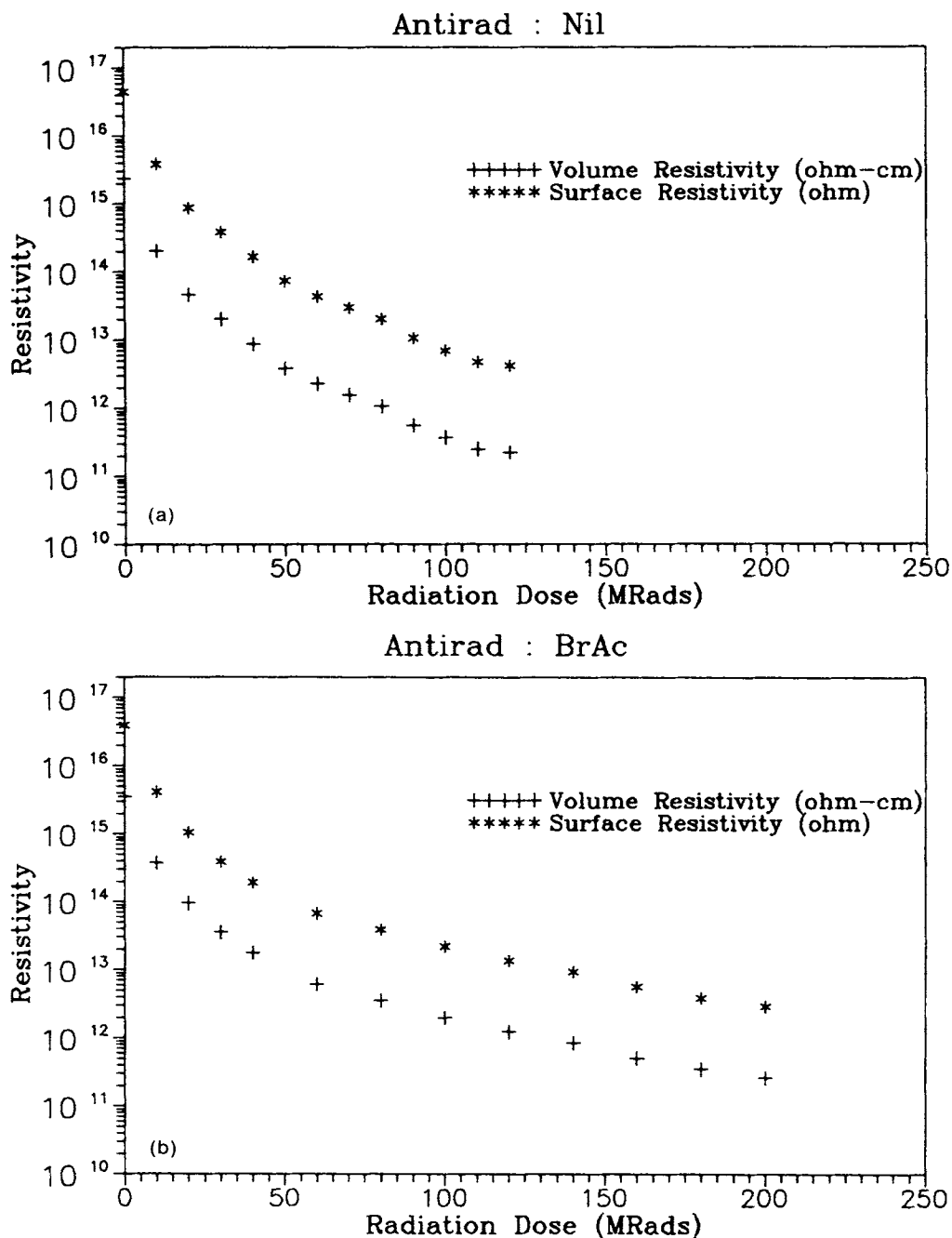


**Figure 3** Plots of volume and surface resistivity at different doses of  $\gamma$  irradiation for EPDM vulcanizates: (a) control, (b) BrAc, (c) pyrene, (d) PAcSu, and (e) PPySu.

The increase in resistivities for all the specimens was found to be negligible beyond 24 h after removal from the  $\gamma$  chamber. Therefore, all specimens subjected to the resistivity studies at different exposed dose were conditioned at room temperature and 55% relative humidity for 24 h for studying the effect of different cumulative dosage of  $\gamma$  radiation.

#### **Radiation Exposure Effects Measurements**

The volume and surface resistivities of specimens are decreased after subjecting them to  $\gamma$  irradiation as can be seen from the Figure 3 [(a)–(e)]. The pronounced effect of antirads is clearly seen by comparing the curves representing the control spec-

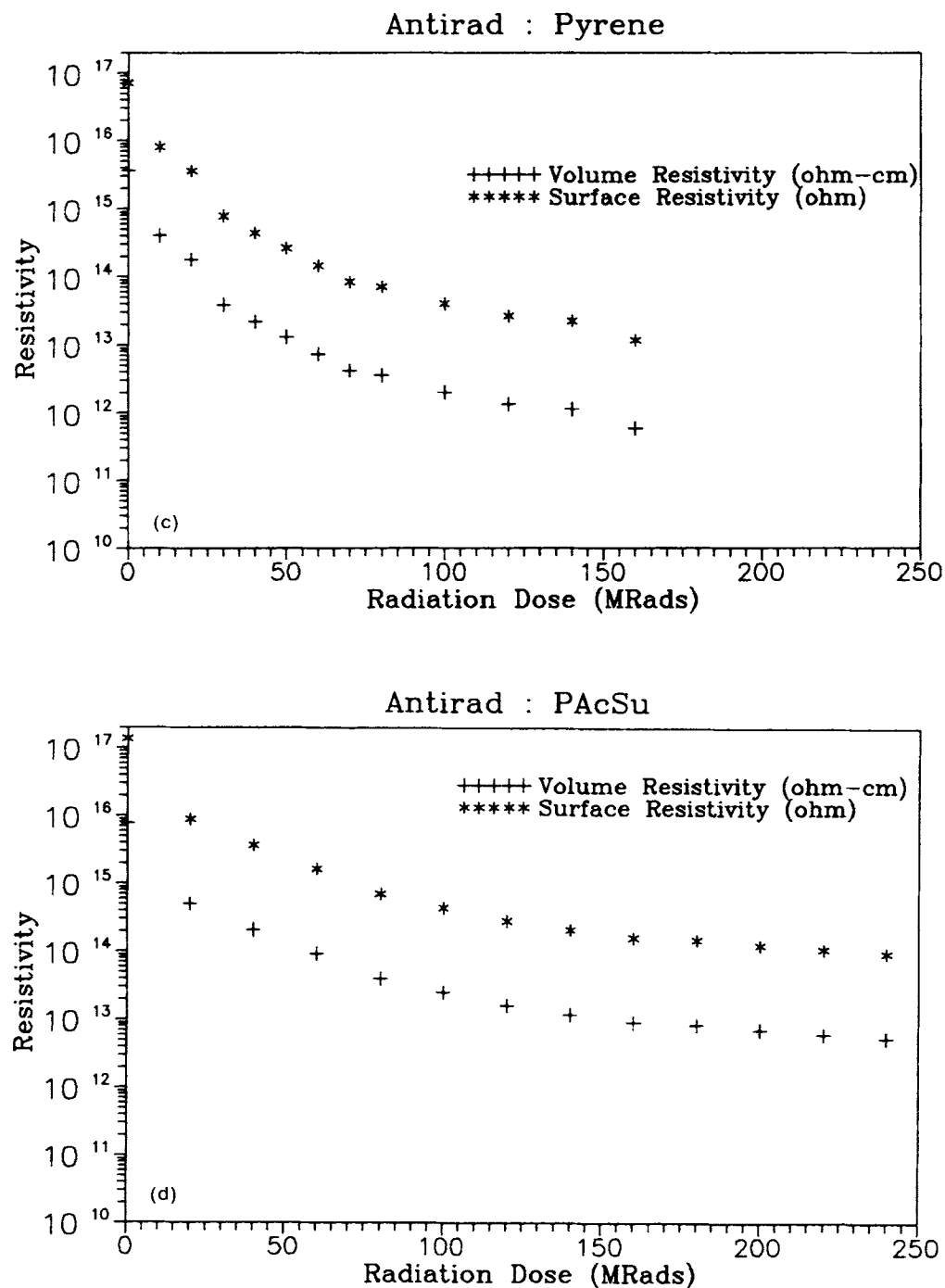


Figure 3 (Continued from the previous page)

imen with those for antirads. The decrease in surface and volume resistivity values is less when antirads are added in the formulations. These can be attributed to the energy scavenging and free radical quenching by antirads. The curves of volume resistivity and surface resistivity for each specimen are almost parallel. This is indicative of homogeneous

changes in the bulk rather than only a surface phenomenon.

The steric hindrance on the antirad molecules does not allow the formation of singlet oxygen to be formed within the bulk during irradiation. This in turn retards the formation of polar species on the backbone chain resulting in the lesser reduction in

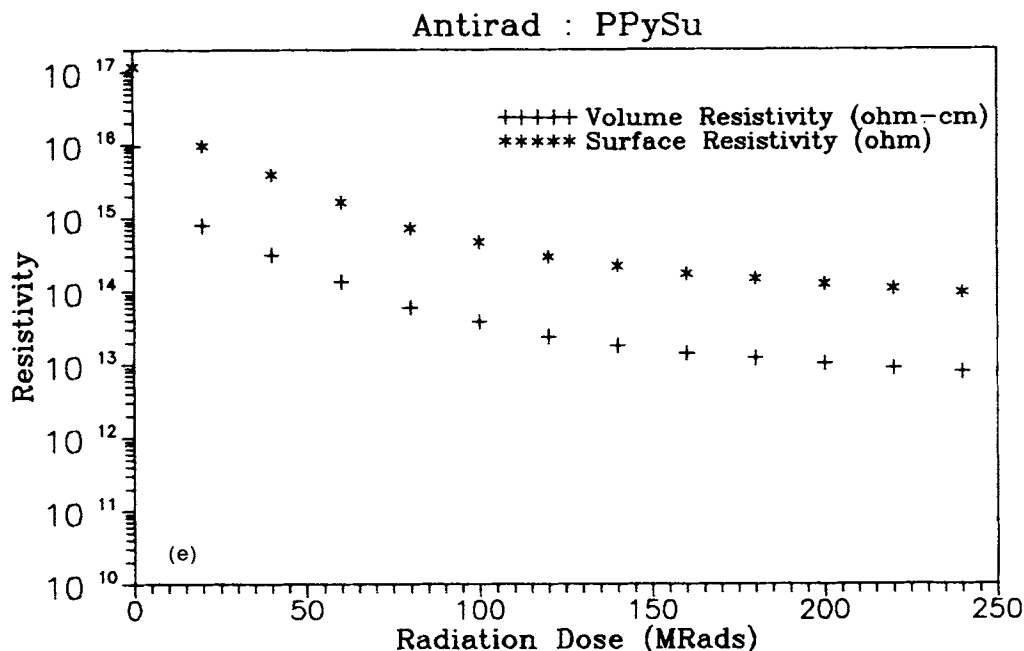


Figure 3 (Continued from the previous page)

the resistivities. The action of energy scavenging and free radical quenching being dependent on the size of the molecule, the efficiency is as expected to be as per the following order:



#### Wide-Angle X-ray Diffraction (WAXD) Spectroscopy

In general, WAXD patterns of all the specimens studied show mainly a halo between  $10^\circ$  to  $30^\circ$   $2\theta$  with a crystalline peak centering at  $21^\circ$   $2\theta$  with several other peaks below and above the halo. The ob-

served crystallinity in EPDM is attributed to high ethylene content (72%) in the polymer.

The radiation-exposed specimens indicate that there are many extra peaks appearing along with reduction in the area of crystalline peak centered at  $21^\circ$  as indicated in the Figure 4. The effect of radiation could be monitored by comparing the percentage crystallinity calculated using the standard procedure<sup>12</sup> from the peak between  $10^\circ$  and  $30^\circ$  of  $2\theta$ . As seen from Figure 5, the percentage crystallinity is reducing with the increase in cumulative exposed dose of  $\gamma$  radiation. These observations may be explained as follows.

The ethylene-rich crystalline zones of polymer, preferentially undergoes crosslinking on exposure to high-energy radiation. The chain mobility restrictions imposed because of the crystallization and the starvation of oxygen in these zones results in intramolecular and interlamellar crosslinking. However, the rate of crosslinking increases only after a prolonged exposure as the recombination rate of the free radicals generated is also high. With the onset of crosslinking in the crystalline zones, the ordered structure starts distorting, ultimately leading to a complete destruction of the ethylene-rich crystallites resulting in the observed decrease in percentage crystallinity. Simultaneously in the propylene-rich amorphous zones, because of the diffused oxygen and easy movements of the chain segments,

Table IV Half-Life Data of Transient Charged Species from dc Resistivity Measurements

Recipe No.	Antirad Used	Half Life <sup>a</sup> (h)	
		(a)	(b)
1	Nil	7.3	7.5
2	BrAc	5.4	5.5
3	Py	4.5	4.7
4	PAcSu	3.5	3.6
5	PPySu	3.2	3.2

<sup>a</sup> (a) Computed from volume dc resistivity measurements; (b) computed from surface dc resistivity measurements.

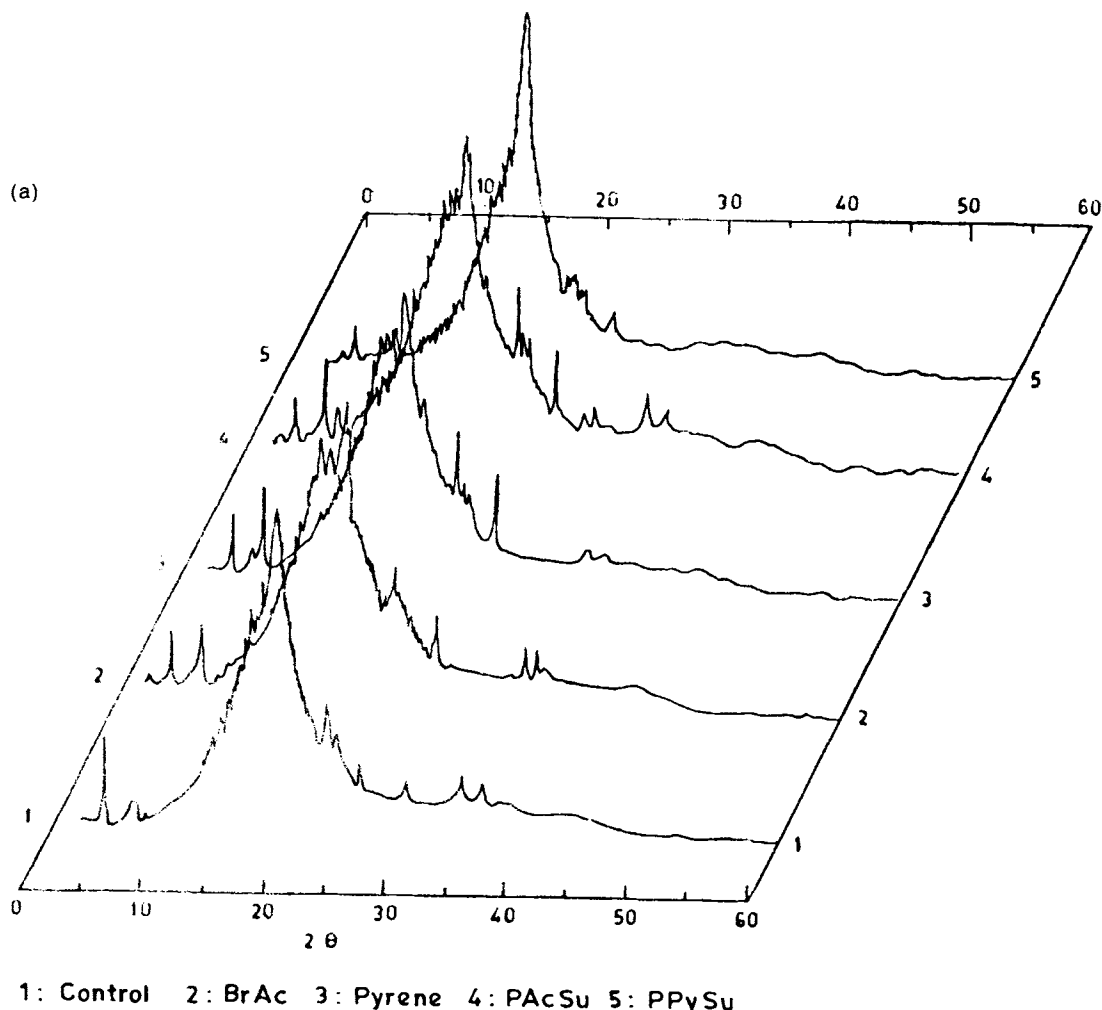


**Figure 4** Plots of wide-angle X-ray diffraction spectra of EPDM vulcanizates: (a) unirradiated vulcanizates, (b) control specimen at different dose of  $\gamma$  irradiation, (c) BrAc specimen at different dose of  $\gamma$  irradiation, and (d) PPySu specimen at different dose of  $\gamma$  irradiation.

the free radicals and the charged species formed have larger life time and are free to undergo mechanism of oxidation and the chain scission. This results in the formation of short-chain segments with polar end groups leading to molecular rearrangements in amorphous zones. However, crosslinking reactions prevail at higher exposed dose because efficiency of crosslinking for ethylene is at least 10-fold more than that for the chain scission in propylene segments. Thus the appearance of extra peaks in the WAXD pattern for the material exposed to very high dose of  $\gamma$  radiation and simultaneous reduction in the crystallinity in control specimen may be explained.

The presence of antirads in the bulk do not affect the morphology as indicated by the Figure 4 (a). The free radical scavenging and oxygen scavenging action

along with energy scavenging mechanism reduce the rate of crosslinking and chain scission. This explains the trend observed in the Figure 5, where in addition of the antirads has dramatically reduced the change in crystallinity with the irradiation dose, giving a clear evidence of the stabilizing action of these antirads.

The order of the stabilization based on the observed data may be presented as follows:

$$\text{Control} < \text{BrAc} < \text{Py} < \text{PACSu} \sim \text{PPySu}$$

### Mechanical Properties

It is very clear from the Figure 6 [(a)–(d)] that the tensile strength and elongation reduce whereas



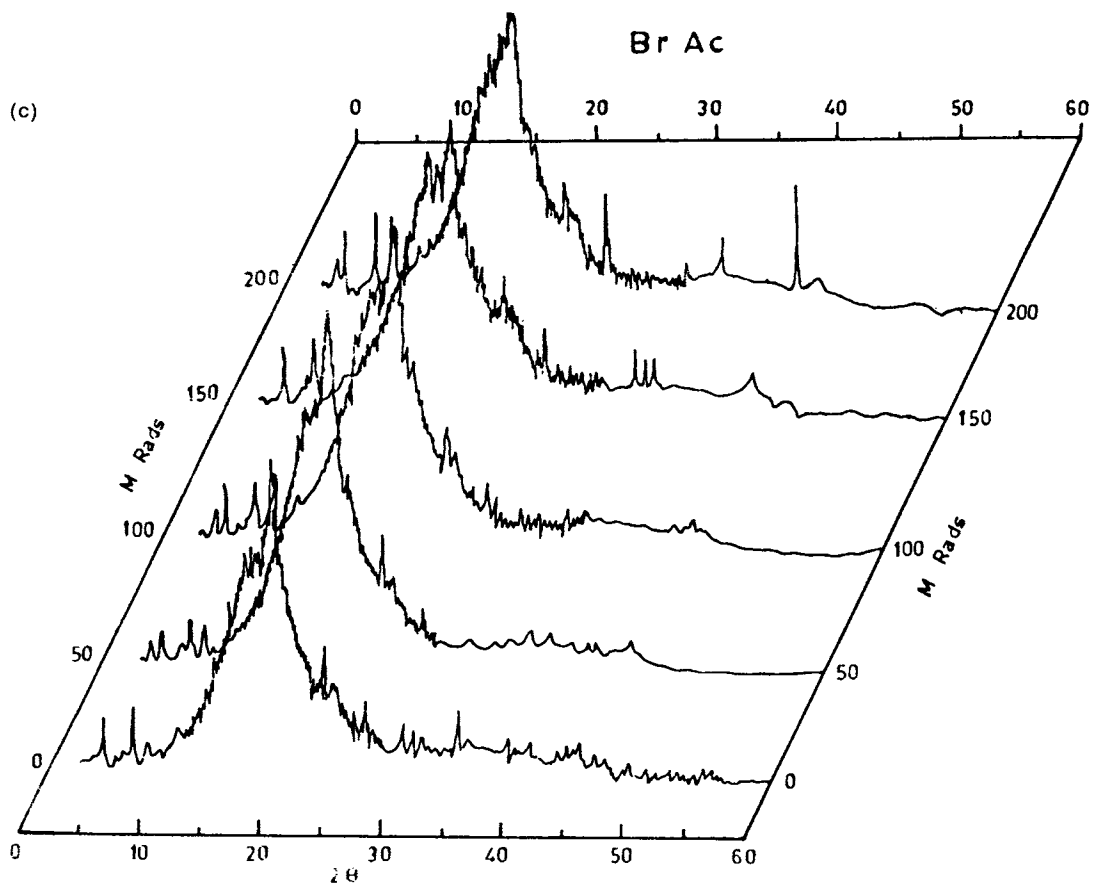
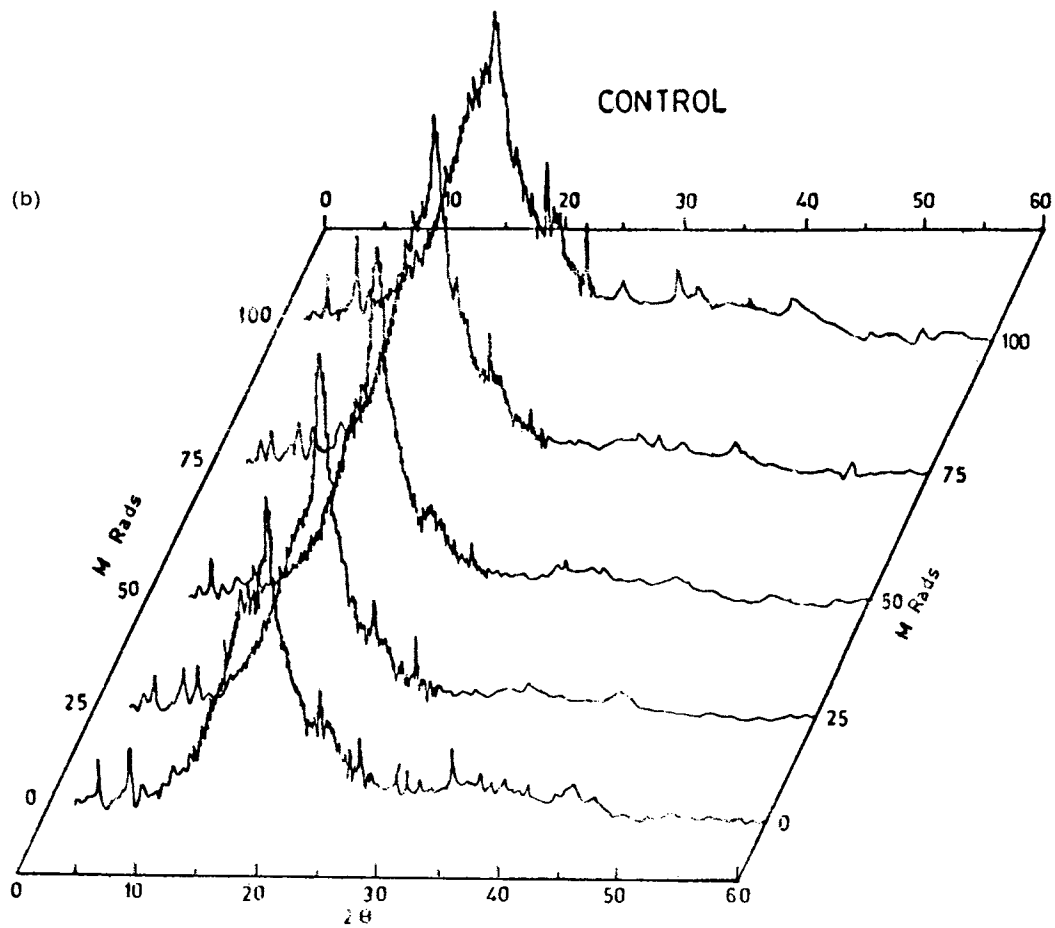


Figure 4 (Continued from the previous page)

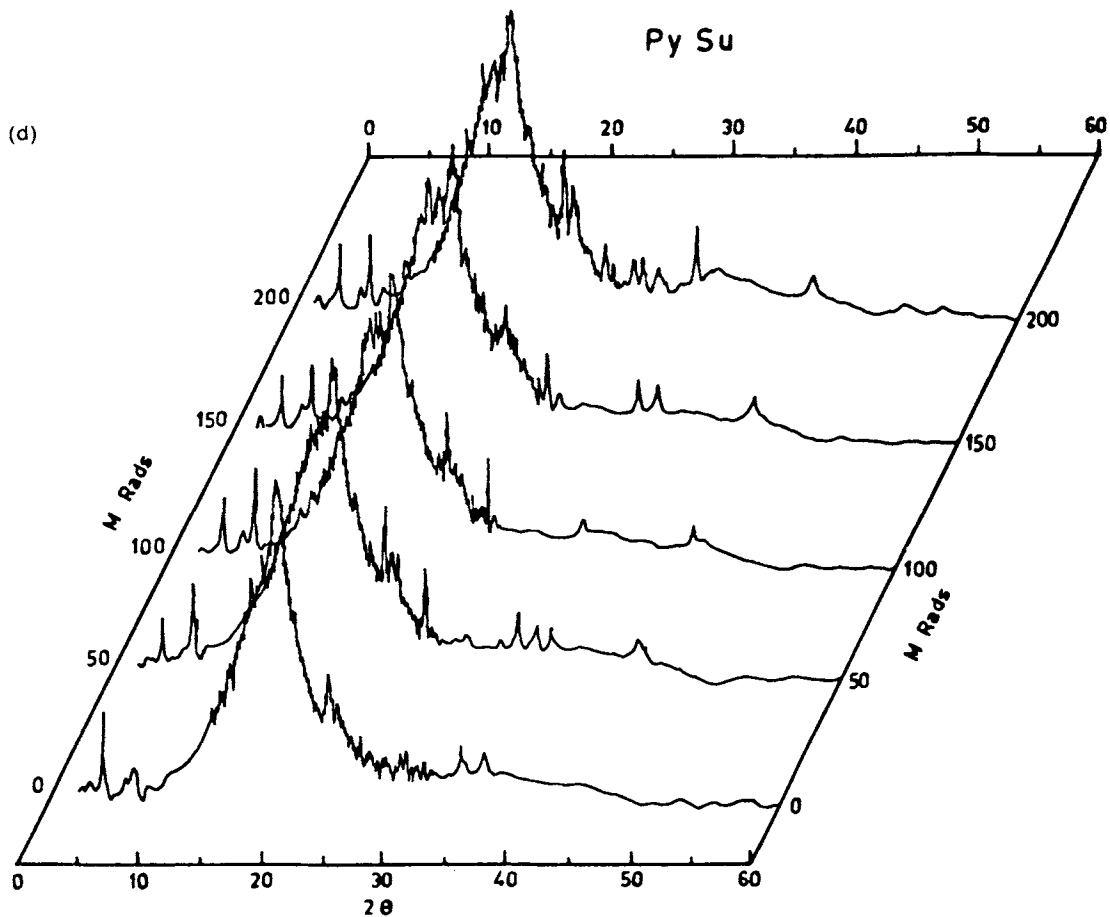


Figure 4 (Continued from the previous page)

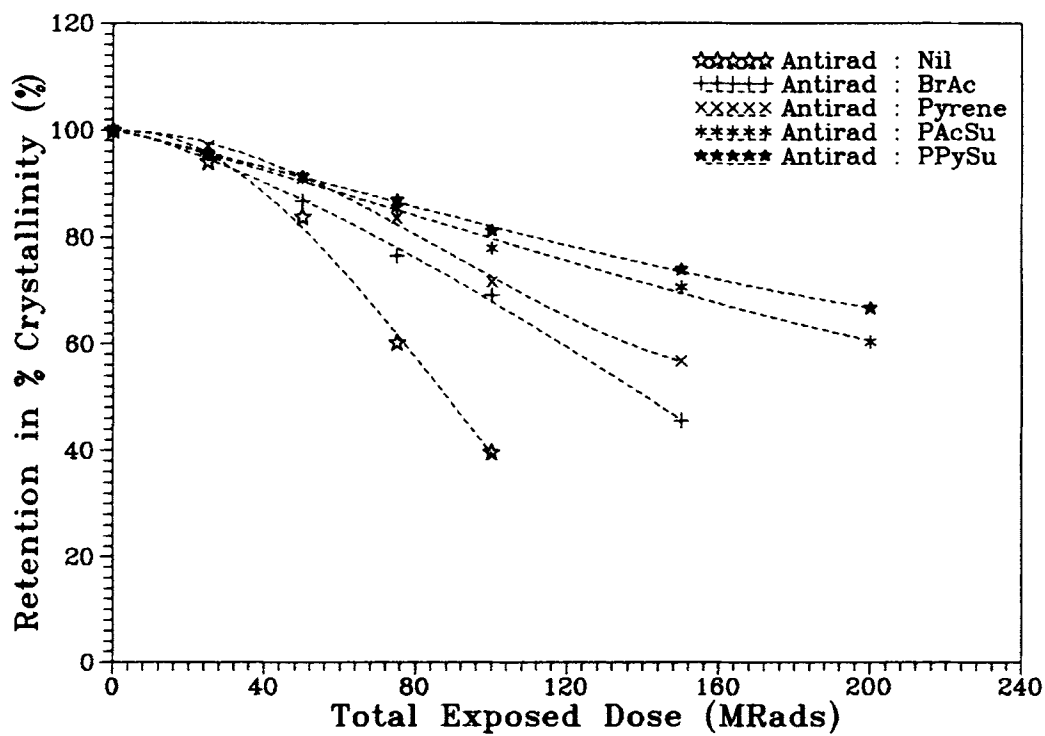


Figure 5 Plots of percentage retention in percentage crystallinity calculated from EPDM crystalline peak with respect to total exposed dose of  $\gamma$  radiation.

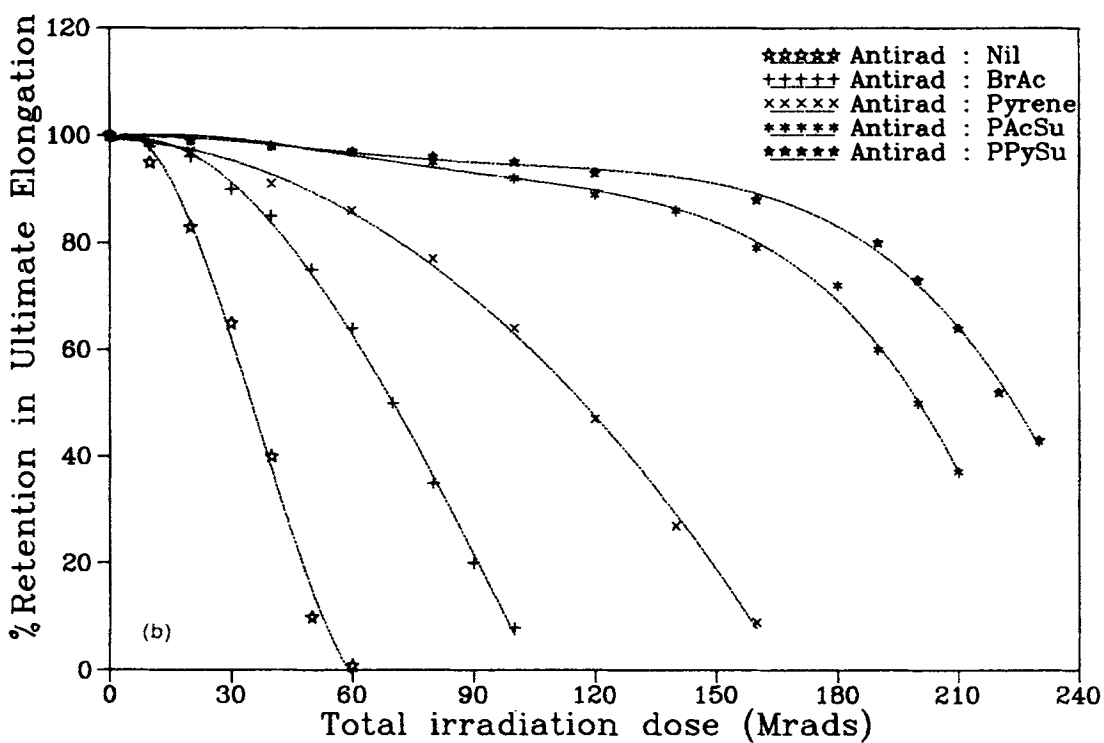
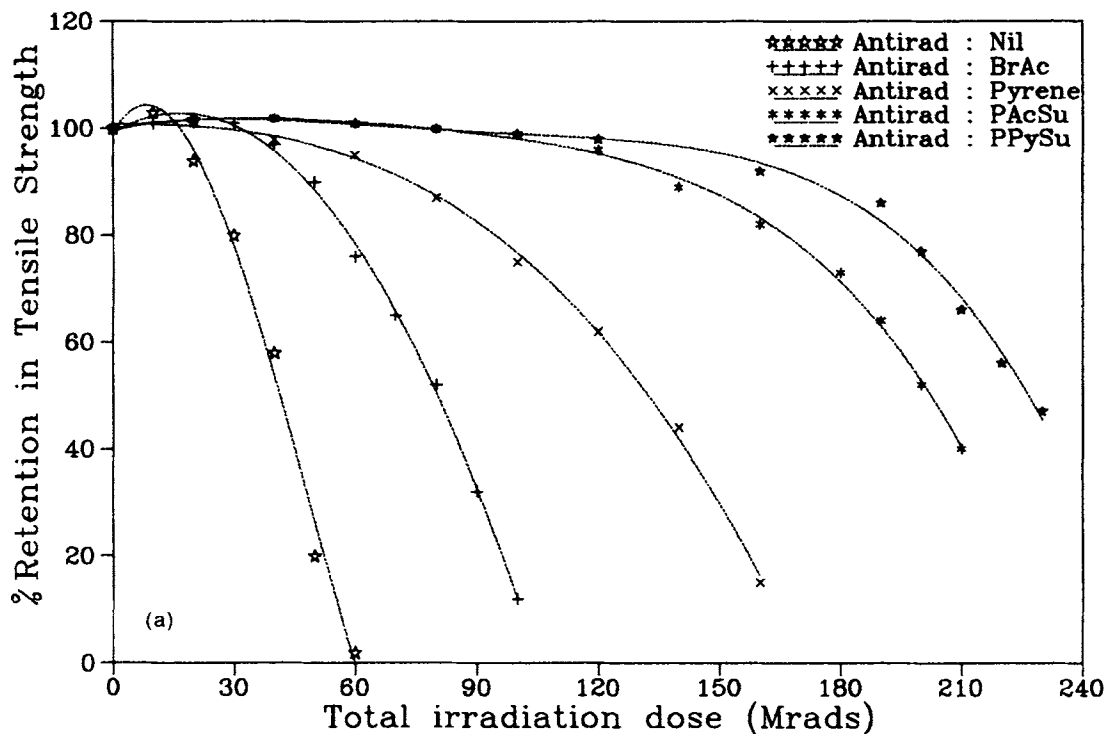


Figure 6 Plots of percentage retention in mechanical properties of EPDM vulcanizates at different dose of  $\gamma$  irradiation: (a) tensile strength, (b) ultimate elongation at break, (c) modulus at 100% elongation, and (d) hardness (shore A).

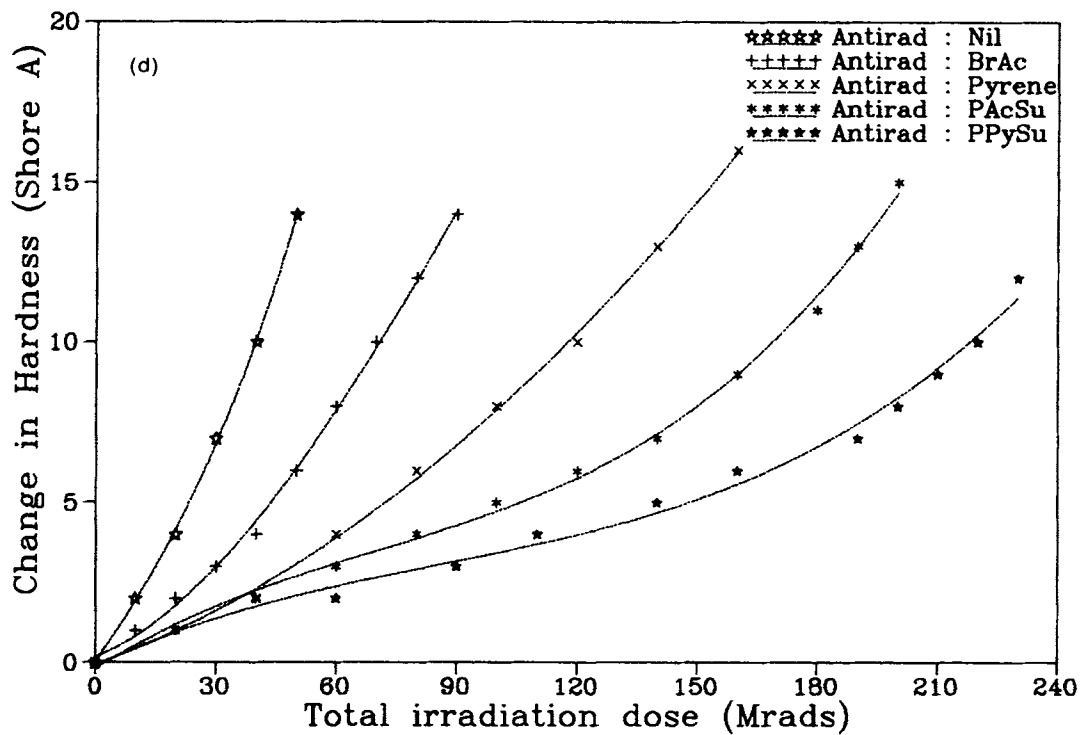
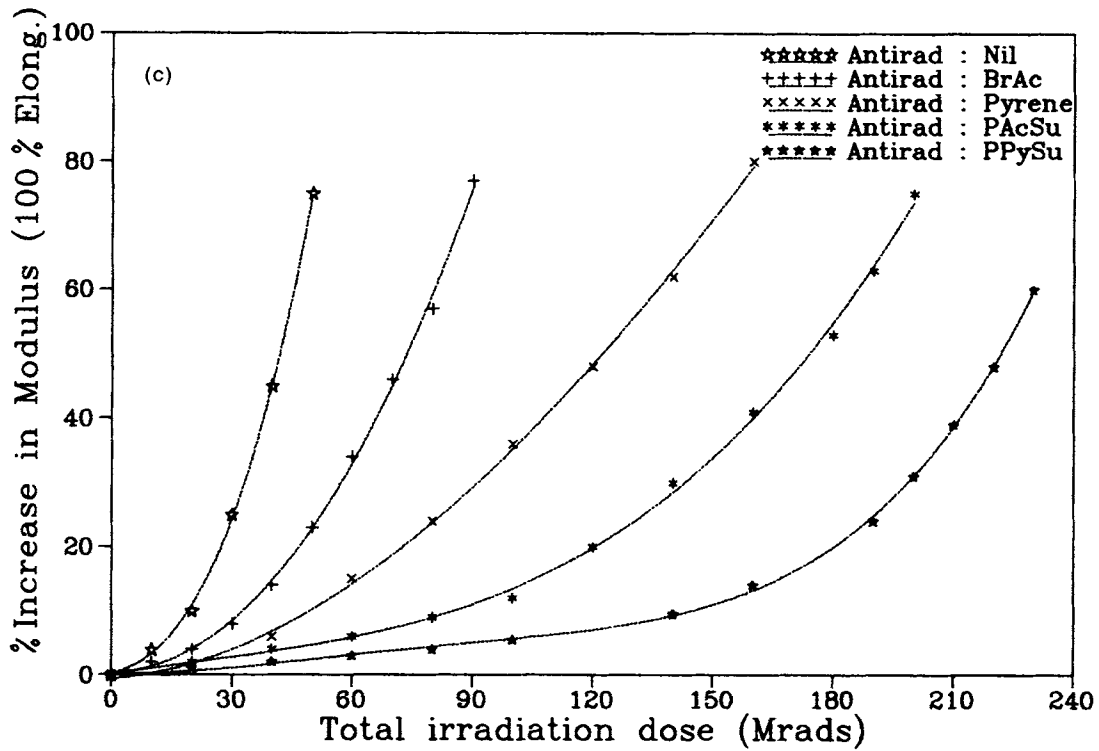


Figure 6 (Continued from the previous page)

modulus and hardness increase with the increased dose of  $\gamma$  radiation. These trends indicate that all the specimens deteriorate predominantly via cross-

linking mechanism. This corroborates the WAXD data and resistivity measurements. However, it can be seen that the deterioration in the properties is

**Table V Failure Criteria Selected for Mechanical Properties<sup>13</sup>**

% Change in tensile strength	50%
% Change in elongation at break	50%
% Change in modulus (at 100% elongation)	50%
Change in hardness	10 units (shore A)

slowed down with the addition of antirads and thereby achieve the necessary mechanical stability criteria. The materials with PPySu and PAcSu antirads satisfy the stability criteria for the material, as defined in the Table V, up to 200 Mrads, where as Py and BrAc stabilizes the material only up to 100 Mrads. Thus the stabilizing action of the antirads can be presented in the following order:



## CONCLUSIONS

The polynuclear compounds used as antirads act as energy scavenger and free radical scavengers in the high-energy radiation environment. Antirads in combination with an antioxidant not only retard the oxidative radiolysis but can also improve the induction period of degradation. The use of polymeric polynuclear aromatics like poly(pyrene sulfide) and poly(acenaphthene sulfide) can enhance the stability up to 200 Mrads very easily. The use of wide-angle X-ray diffraction analysis provides evidence of EPDM undergoing degradation predominantly via crosslinking reactions. The dc resistivity mea-

surements and wide-angle X-ray diffraction analysis established the following order of antirad efficiency: brominated acenaphthene < pyrene < poly(acenaphthene sulfide) ~ poly(pyrene sulfide).

## REFERENCES

1. F. P. Baldwin and G. Ver Strate, *Rubber Chem. Technol.*, **45**, 709 (1972).
2. S. Cesca, *Macromol. Rev.*, **10**, 1 (1975).
3. I. Kuriyama, N. Hayakawa, Y. Nakase, S. Kawawata, J. Ogura, and K. Kasai, *IEEE Trans. Electr. Insul.*, **EI14**, 272 (1979).
4. I. Kuriyama, N. Hayakawa, Y. Nakase, S. Kawawata, J. Ogura, K. Kasai, and T. Onishi, *IEEE Trans. Electr. Insul.*, **EI13**, 164 (1978).
5. Y. Nakase and M. Ito, *IEEE Trans. Electr. Insul.*, **EI16**, 528 (1981).
6. R. L. Clough and K. T. Gillen, *Polym. Degrad. Stabl.*, **30**, 309 (1990).
7. J. B. Gardner and B. G. Harper, *J. Appl. Polym. Sci.*, **9**, 1965 (1985).
8. K. Wundrich, *J. Polym. Sci., Polym. Phys. Ed.*, **12**, 201 (1974).
9. C. S. Shah, M. J. Patni, and M. V. Pandya, *Frontiers of Polymer Research*, Ed., P. N. Prasad and J. K. Nigam, Plenum Press, New York, 1991, p. 565.
10. C. S. Shah, M. J. Patni, M. V. Pandya, and M. R. Desai, *J. Appl. Polym. Sci.*, **51**, 1505 (1994).
11. F. A. Makhlis, *Radiation Physics and Chemistry of Polymers*, Halsted Press, New York, 1975, p. 127.
12. F. W. Billmeyer, Jr., *Textbook of Polymer Science*, Wiley, Singapore, 1984, p. 288.
13. IEC Standard 544.

Received June 11, 1993

Accepted January 22, 1994